European Journal of Medicinal Chemistry 45 (2010) 1760–1771

Contents lists available at ScienceDirect

European Journal of Medicinal Chemistry

journal homepage: http://www.elsevier.com/locate/ejmech

Original article

Synthesis, pharmacological activity and comparative QSAR modeling of 1,5-*N*,*N*′-substituted-2-(substituted naphthalenesulphonyl) glutamamides as possible anticancer agents

Amit Kumar Halder [1], Nilanjan Adhikary, Milan Kumar Maity, Tarun Jha*

Natural Science Laboratory, Medicinal and Pharmaceutical Chemistry, Department of Pharmaceutical Technology, P.O. Box 17020, Jadavpur University, Kolkata 700 032, India

ARTICLE INFO

Article history:
Received 18 August 2009
Received in revised form
4 January 2010
Accepted 6 January 2010
Available online 21 January 2010

Keywords:
Glutamamide
EAC
Anticancer activity
Comparative QSAR
Wang-Ford charge

ABSTRACT

Based on our earlier QSAR study, a series of 1, 5-N,N′-substituted-2-(substituted naphthalenesulphonyl) glutamamides were synthesized as possible anticancer agents. Anticancer activities of these synthesized compounds were evaluated in vivo on Swiss Albino mice against Ehrlich Ascites Carcinoma (EAC) cells where inhibitions of tumor cell and tumor weight were considered as biological activity parameters. A comparative QSAR study was done with a set of descriptors and logarithm of tumor cell inhibition. The result shows the importance of topological parameters like ETSA and RTSA indices as well as electronic parameter like Wang-Ford charges of different atoms. Electrophilic attack at atom number 5 and increased number of chlorine atom may be favorable whereas presence of methoxy group at the atom number 8 in naphthalene ring may be detrimental to the activity.

© 2010 Elsevier Masson SAS. All rights reserved.

1. Introduction

Glutamine is considered as an essential ingredient for growth of tissues. It is an important nutrient for rapidly growing cells [1–7]. It also plays a key role in tumor growth. It acts as one of the major substrates [6–8] in cancer. Some cancer cells require higher glutamine concentrations than normal cells. Glutamine plays a key role in cell growth by supplying its amide nitrogen atoms in the biosynthesis of other amino acids and purine and pyrimidine bases and, thus, is involved in both DNA and protein syntheses, Hence, it may may have influence to alter the genetic code of protein syntheses and may lead to cancerous proteins which may be slightly different from their normal counterparts [9–11]. The balance between glutamine formation and utilization relies largely on the activity of two enzymes namely glutaminase and glutamine synthetase. In mitochondria, glutamine is acted upon by glutaminase. This enzyme requires high phosphate concentration to be fully active. Moreover, tumor glutaminase reaches a maximum expression and activity immediately before the maximum proliferation rate of tumor cells. It is indicative of the vital role of this enzyme in tumor growth. On the other hand, glutamine synthetase is also considered as 'dispensable enzyme' for tumor [11–15]. In keeping with these facts, some derivatives and analogs of glutamamide were synthesized as a part of our composite programme of drug design and discovery [16–23]. In the present article, we have reported of synthesis of some glutamamide analogs that are structural derivatives of both glutamine and glutamic acid. Our previous QSAR study on thirty two 1,5-*N*,*N*′-disubstituted-2-(substituted benzenesulphonyl) glutamamides [23] showed that the increase in the number of benzene ring in the structure may be helpful for increasing the activity of these compounds. Based on this assumption, we have considered fused benzene ring or naphthalene ring in the present article we synthesized twenty eight 1,5-*N*,*N*′-disubstituted-2-(substituted naphthalenesulphonyl) glutamamides. These were subsequently characterized and biologically evaluated using *in vivo* anticancer model. Some of these synthesized compounds have shown considerable biological activity. Hence, in order to further investigate the chemical structural features of these compounds, QSAR studies were performed. For the QSAR study, *in vivo* anticancer activity data of inhibition of cell count was used as the dependent parameter. Physicochemical, topological, quantum chemical and constitutional descriptors were calculated. These were subsequently treated as the independent parameters. Three different statistical methods: principal component regression analysis (PCRA), stepwise regression and factor

* Corresponding author. Tel.: +91 33 24146666x2495 (office), +91 33 24383814 (residencial), 09433187443 (mobile); fax: +91 33 24146927.
E-mail address: tjupharm@yahoo.com (T. Jha).
[1] Present address: Dr. B. C. Roy College of Pharmacy and Allied Health Sciences, Dr. M. S. Sarani, Bidhannagar, Durgapur, West Bengal, India.

0223-5234/$ – see front matter © 2010 Elsevier Masson SAS. All rights reserved.
doi:10.1016/j.ejmech.2010.01.008

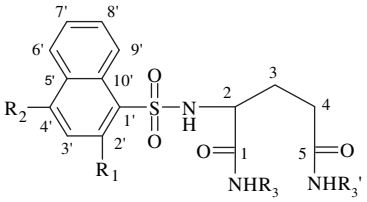

Fig. 1. General structure of 1,5-*N*,*N*′-disubstituted-2-(substituted naphthalenesulphonyl) glutamamides (**17**–**44**).

analysis-multiple linear regression (FA-MLR) were used for the development of comparative QSAR models. All QSAR models showed significant statistical qualities. The general structure of 1,5-*N*,*N*′-disubstituted-2-(substituted naphthalenesulphonyl) glutamamides (**18**–**45**) is shown in Fig. 1.

2. Chemistry

Substituted naphthalenesulphonyl chlorides (**5**–**8**) were synthesized by chlorosulphonylation of naphthalene and naphthalene derivatives (**1**–**4**). These were first separately dissolved in dry chloroform. The naphthalene ring is susceptible to disubstitution at higher temperature. Cold temperature (0–5 °C) was always maintained during chlorosulphonylation process. 2-(substituted naphthalenesulphonyl)-L(+) glutamic acids (**10**–**13**) were prepared by condensing L(+)-glutamic acid (**9**) with substituted naphthalenesulphonyl chlorides separately. In this reaction, alkaline medium (2 N NaOH) was maintained to remove hydrochloric acid which was continuously formed during the condensation reaction. As chlorine and bromine are deactivating groups, reaction temperature was maintained around 85–90 °C during the condensation. It helps to get better yield otherwise 65–70 °C temperature was maintained in Schotten–Baumann reaction as reported earlier [23]. 2-(substituted naphthalenesulphonyl)-L(+) glutamic acids were subsequently refluxed separately with thionyl chloride in order to produce corresponding dichloride derivatives (**14**–**17**). Neucleophilic displacement of chloro-groups of 2-(substituted naphthalenesulphonyl) glutamic acids dichloride (**14**–**17**) with different amines yielded the corresponding diamides (**18**–**45**) which were the title compounds. The crude compounds were recrystallised from dilute ethanol. The general structures of starting material and intermediates as well as synthetic scheme are given in Fig. 2.

3. Pharmacology

Anticancer activity of these synthesized title compounds (**18**–**45**) were evaluated by *in vivo* method. The method was standardized in our laboratory [16–23]. Antitumor activities of twenty eight synthesized glutamamides were evaluated by either dissolving these compounds in phosphate buffered saline (PBS) or by suspending in PBS with 2% Tween 80 (where and when necessary) separately. These were used with a dose 2 mmol/Kg/day against Ehrlich Ascites Carcinoma (EAC) cells impregnated in Swiss Albino mice. Percentage tumor cell inhibition (% TCI) and percentage tumor weight inhibition (% TWI) were used as biological activity parameters. These parameters were obtained by the following expressions:

$$\text{Percentage inhibition of Ascites cells} = (1 - T/C) \times 100$$
$$\text{Percentage inhibition of Ascites fluid} = (1 - T'/C') \times 100$$

where T is the mean number of Ascitic cells/ml in test animals, C is the mean number of Ascitic cells/ml in control animals, T' is the mean weight of Ascitic fluid in test animals and C' is the mean weight of Ascites fluid in control animals.

In the present study, Mitomycin C was chosen as the universal standard drug and azaserine as well as DON as specific standards to compare the activity of the test compounds. These were dissolved separately in sterile phosphate buffer (pH 7.2). Standards were administered separately at a dose level of 1 mg/kg body weight. These showed 100% inhibition in both cell count and tumor weight.

4. QSAR study

A comparative QSAR study [24,25] of these twenty eight synthesized 1,5-*N*,*N*′-substituted-2-(substituted naphthalenesulphonyl) glutamamides were performed using percentage tumor cell inhibition (% TCI) as the biological activity parameters.

4.1. Dataset and parameters

A large dataset of various physicochemical, topological and semi-empirical quantum chemical descriptors were calculated by using different softwares. While calculating these descriptors, arbitrary numbering of the pharmacophore was done for all atom level calculations. This arbitrary numbering is shown in Fig. 3.

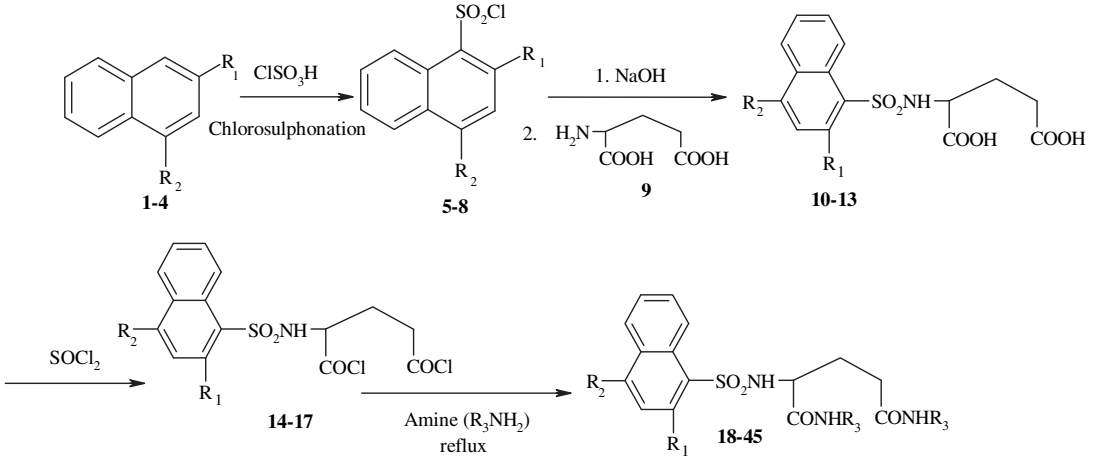

Fig. 2. Scheme for synthesis of title compounds.

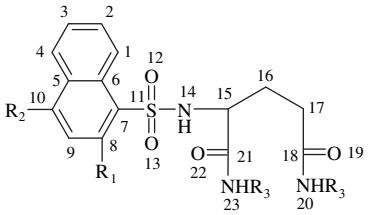

Fig. 3. General structure for QSAR with arbitrary numbering.

Apart from these, indicator parameters were also used in order to find out the role of the specific substituent at a particular position towards the biological activity. Parameters used to develop QSAR equations were the standardized by using Eq. (1):

$$X_{ki} = (xi - xi_{minimum})/(xi_{maximum} - xi_{minimum}) \quad (1)$$

The standardized values of the descriptors appeared in the QSAR models are provided in Supplementary Material.

4.2. Statistical methods

Three statistical methods-stepwise multiple linear regression (sMLR), factor analysis-multiple linear regression (FA-MLR) and principle component regression analysis (PCRA) were used separately for development of QSAR models. These are briefly described below in the following sections:

4.2.1. Principle component regression analysis (PCRA)

In PCRA [26–29], factor scores were obtained from factor analysis on the data matrix containing all the independent variables. Factor analysis was performed after VARIMAX rotation. Regression analysis was performed considering factor scores as predictor variables. As factor score contains information for different descriptors, the chance for loss of information is less.

4.2.2. Stepwise regression method

In stepwise regression, multiple linear equations were developed step by step [26]. A primary stepping criteria based on F values was imposed on the system. Predictor variables were added or removed according to these stepping criteria. The search was terminated when the stepping was no longer possible.

4.2.3. Factor analysis-multiple linear regression (FA-MLR)

In FA-MLR [29], principle component method was used to extract these factors. Then it was rotated by VARIMAX rotation. The goal of factor analysis was to represent the multidimensional data matrix in low dimensional space with minimum loss of information. The aim of VARIMAX rotation was to maximize the variance of the new variable. This also helps to reduce the variance around the new variable. Factor pattern suggested whether the biological activity could be explained satisfactorily within the parameter space or not.

Statistical qualities of MLR equations were judged by correlation coefficient (R), adjusted R^2 (R^2_A), variance ratio (F), probability factor related to F-ratio (p) and standard error of estimate (s).

4.2.4. Validation of the QSAR models

Leave-One-Out (LOO) cross-validation method was used to validate the predictive powers of all MLR, FA-MLR, PCRA and PLS equations. The predicted residual sum of square (PRESS), total sum of squares (SSY), cross validated R^2 (R^2_{cv}), standard deviation error of prediction (SDEP) and standard error of PRESS (S_{PRESS}) were considered for validations of QSAR models.

5. Results

Synthesized 1,5-*N*,*N*′-substituted-2-(substituted naphthalenesulphonyl) glutamamides were obtained as crystalline solids with appreciable yields. Biological activities of these compounds are given in Table 1. Table 1 suggests that these synthesized compounds have variable anticancer activities. For the present QSAR analysis, the percentage EAC cell inhibition (% TCI) of these synthesized compounds was considered as the biological activity parameter. Thus, all % TCI values were converted to logarithmic scales. These were subsequently used as dependent variables.

The results obtained by different statistical analyses are shown below:

5.1. Principal component regression analysis (PCRA)

In PCRA, ten factor scores were extracted by principle component method. Then, it was rotated by VARIMAX rotation. These factor scores were used as independent parameters for developing QSAR equations. Using forward selection method, the following equation was developed:

$$\begin{aligned}\log BA &= 1.448(\pm0.035) - 0.100(\pm0.036)f_1 \\ &\quad +0.063(\pm0.036)f_3 - 0.070(\pm0.036)f_4 \\ &\quad -0.134(\pm0.036)f_7 - 0.160(\pm0.036)f_8 \\ n &= 28;\ R = 0.829;\ R^2 = 0.687;\ R^2_A = 0.616;\ F(5,22) \\ &= 9.6782;\ p < 0.00005;\ S.E.E = 0.186;\ R^2_{cv} \\ &= 0.492;\ SSY = 2.442;\ PRESS = 1.240;\ SDEP \\ &= 0.210;\ S_{PRESS} = 0.237. \end{aligned} \quad (2)$$

Where n is the number of data points. The 95% confidence intervals of the regression coefficients are shown in parentheses.

5.2. Stepwise regression

Using stepping criteria on the basis of F value ($F = 3.0$ for inclusion; $F = 2.9$ for exclusion), the QSAR equation was derived with six variables. The best found stepwise regression equation is given in Eq. (3):

$$\begin{aligned}\log BA &= -28.316(\pm5.035) + 0.449(\pm0.173)\, f^{(E)}5 \\ &\quad +8.782(\pm1.191)q_{14} - 16.474(\pm3.060)q_{19} \\ &\quad -4.394(\pm0.737)S_{15} - 8.1267(\pm1.526)q_{12} \\ &\quad +2.6601(\pm0.577)R_{17} \\ n &= 28;\ R = 0.906;\ R^2 = 0.821;\ R^2_A = 0.770;\ F(6,21) \\ &= 16.106;\ p < 0.00001;\ S.E.E = 0.144;\ R^2_{cv} \\ &= 0.657;\ SSY = 2.442;\ PRESS = 0.837;\ SDEP \\ &= 0.173;\ S_{PRESS} = 0.199. \end{aligned} \quad (3)$$

Where $f^{(E)}5$ is the frontier electron density for electrophilic attack at the atom number 5. q_{12}, q_{14} and q_{19} are Wang-Ford charges of atom numbers 12, 14 and 19 respectively. S_{15} is the ETSA index of the atom number 15. R_{17} is the R-state index of the atom number 17.

5.3. Factor analysis-multiple linear regression (FA-MLR)

Factor analysis was performed after VARIMAX rotation as data preprocessing step. It helps to select descriptors for QSAR

Table 1
Biological activity data of synthesized compounds.

Cpd[a]	Mean wt. of Ascitic fluid in control (gm)	Mean wt. of Ascitic fluid in Test (gm)	% Inhibition of Ascitic fluid (TWI)	Mean no of cells/ml in control × 10^5	Mean no. of cells/ml in Test × 10^5	% inhibition of ascitic cell (TCI)
18	1.917 (±0.325)	1.300 (±0.198)	32.19	433.82 (±3.623)	267.49 (±2.152)	38.34
19	2.066 (±0.230)	1.500 (±0.216)	27.42	299.63 (±3.150)	91.92 (±3.280)	69.32
20	2.166 (±0.228)	1.633 (±0.224)	24.61	482.84 (±2.588)	348.04 (±1.942)	27.92
21	2.166 (±0.228)	1.817 (±0.117)	16.15	482.84 (±2.588)	414.22 (±1.877)	14.21
22	2.066 (±0.230)	1.700 (±0.156)	17.74	299.63 (±3.150)	197.3 (±1.677)	43.96
23	1.917 (±0.325)	1.642 (±0.124)	14.34	433.82 (3.623)	363.67 (2.635)	16.17
24	2.066 (±0.230)	1.820 (±0.114)	11.93	299.63 (±3.150)	113.97 (±1.814)	61.96
25	2.767 (±0.142)	1.200 (±0.328)	56.62	373.77 (±1.582)	307.83 (±2.366)	17.64
26	1.920 (±0.228)	1.088 (±0.428)	43.58	439.95 (±4.073)	203.43 (±3.141)	53.76
27	2.025 (±0.336)	1.680 (±0.216)	17.04	416.05 (±3.733)	272.67 (±1.540)	34.46
28	1.920 (±0.228)	0.86 (±0.258)	55.21	439.95 (±4.073)	239.11 (±3.126)	48.52
29	1.920 (±0.228)	1.525 (±0.125)	20.57	439.95 (±4.048)	235.29 (±3.723)	46.52
30	2.240 (±0.420)	1.700 (±0.208)	24.10	439.34 (±4.048)	225.49 (±2.757)	48.67
31	2.240 (±0.420)	1.820 (±0.197)	18.73	439.34 (±4.048)	266.54 (±2.097)	39.33
32	2.235 (±0.218)	1.683 (±0.356)	24.68	399.81 (±3.726)	313.84 (±3.228)	75.17
33	1.917 (±0.325)	1.520 (±0.258)	20.71	433.82 (±3.623)	290.22 (±3.256)	33.10
34	2.240 (±0.420)	1.900 (±0.129)	15.20	439.34 (±4.048)	257.97 (±1.946)	41.28
35	2.025 (±0.336)	1.702 (±0.126)	15.95	416.05 (±3.733)	205.88 (±1.566)	50.51
36	2.025 (±0.336)	1.675 (±0.142)	22.69	416.05 (±3.733)	320.59 (±3.301)	22.94
37	2.235 (±0.218)	1.420 (±0.384)	36.46	399.81 (±3.726)	166.91 (±4.248)	58.25
38	2.235 (±0.218)	1.775 (±0.310)	20.58	399.81 (±3.726)	357.35 (±3.439)	10.62
39	1.520 (±0.410)	1.150 (±0.398)	24.34	452.73 (±4.473)	379.29 (±2.049)	16.22
40	1.520 (±0.410)	1.475 (±0.108)	2.96	452.73 (±4.473)	385.42 (±2.691)	14.86
41	2.767 (±0.142)	2.133 (±0.136)	22.81	373.77 (±1.582)	334.82 (±1.122)	10.42
42	1.520 (±0.410)	1.383 (±0.198)	8.99	452.73 (±4.473)	346.32 (±4.720)	23.50
43	2.120 (±0.421)	1.960 (±0.136)	7.57	422.79 (±3.710)	346.32 (±2.740)	18.78
44	2.120 (±0.421)	1.833 (±0.444)	13.52	422.79 (±3.710)	404.41 (±2.657)	4.34
45	2.120 (±0.421)	2.010 (±0.118)	5.19	422.79 (±3.710)	360.26 (±2.805)	14.79
Mit[b]	2.166 (±0.228)	0.000 (±0.020)	100.00	482.64 (±2.588)	0.000 (±0.050)	100.00
Aza[c]	2.025 (±0.336)	0.000 (±0.230)	100.00	416.03 (±3.733)	0.000 (±0.045)	100.00
DON	2120 (±0.421)	0.000 (±0.300)	100.00	422.79 (±3.710)	0.000 (±0.050)	100.00

[a] Compound.
[b] Mitomycin.
[c] Azaserine.

equations. It was observed that ten factors could explain the data matrix to the extent of 94.5%. The factor loading of significant variables is provided as Supplementary Material. Factor loadings greater that 0.6 are shown in bold face. The biological activity was highly loaded with factor 8 (loaded with S_8, R_8, q_8, I_1 and $f^{(E)}5$) and factor 7 (loaded with q_{18}, q_{19}, *IC*3, *IC*4 and *IC*5). It was intermediately loaded with factor 1 [highly loaded with S_{12}, S_{13}, S_{14}, S_{19}, S_{22}, R_{12}, R_{13}, R_{16}, R_{17}, R_{18}, R_{19}, R_{21}, R_{22}, *Ms*, *SA*(*G*), Vol, log*P*, *Refr*, *Pol*, *SIC*0, *IC*1, *SIC*1, *SIC*2 and *SIC*3], factor 4 (highly loaded with R_1, R_2, R_3, R_4, R_5, R_6, R_9, R_{14} and *n*Br) and factor 3 (S_1, S_3, S_4, S_5, S_6, S_9, S_{10}, q_2, q_4 and *n*Cl), poorly loaded with factor 6 (loaded with S_{15}, S_{16}, S_{17} and HE), factor 5 (loaded with q_{15}, q_{21}, $f^{(E)}18$, $f^{(E)}19$ and $f^{(E)}20$) and factor 10 (loaded with *IC*2). It was very poorly loaded with factor 2 and factor 9. Different combinations of parameters having factor loading of more than 0.6 (excluding very poorly loaded factors) were subjected to multiple linear regression. Intercorrelated parameters were not considered for the development of equations. The results evolved Eq. (4) with five descriptors:

$$\begin{aligned}\log \mathrm{BA} &= -20.435(\pm 3.692) - 0.109(\pm 0.027)R_{10} \\ &\quad +5.711(\pm 0.931)R_{15} + 3.675(\pm 0.662)q_{14} \\ &\quad +8.255(\pm 1.554)q_{18} + 0.968(\pm 0.185)f^{(E)}5 \\ n &= 28;\ R = 0.887;\ R^2 = 0.786;\ R^2_{\mathrm{A}} = 0.738;\ F(5,22) \\ &= 16.188;\ p < 0.00001;\ \mathrm{S.E.E} = 0.154;\ R^2_{\mathrm{cv}} \\ &= 0.670;\ \mathrm{SSY} = 2.442;\ \mathrm{PRESS} = 0.806;\ \mathrm{SDEP} \\ &= 0.169;\ S_{\mathrm{PRESS}} = 0.191. \end{aligned} \quad (4)$$

Where, R_{10} and R_{15} are RTSA indices of atom numbers 10 and 15 respectively. q_{14} and q_{18} are Wang-Ford charges of atom number 14 and 18 respectively.

Another model obtained as:

$$\begin{aligned}\mathrm{Log\ BA} &= 13.733(\pm 1.963) - 1.013(\pm 0.152)S_{12/13} \\ &\quad -0.198(\pm 0.053)R_8 - 5.544(\pm 0.988)q_{17} \\ &\quad +0.327(\pm 0.067)nCl + 1.111(\pm 0.202)f^{(E)}5 \\ n &= 28;\ R = 0.890;\ R^2 = 0.793;\ R^2_{\mathrm{A}} = 0.746;\ F(5,22) \\ &= 16.849;\ p < 0.00001;\ \mathrm{S.E.E} = 0.152;\ R^2_{\mathrm{cv}} \\ &= 0.608;\ \mathrm{SSY} = 2.442;\ \mathrm{PRESS} = 0.960;\ \mathrm{SDEP} \\ &= 0.147;\ S_{\mathrm{PRESS}} = 0.208. \end{aligned} \quad (5)$$

$S_{12/13}$ is the E-state index of the atom number 12 or 13 (as these have same calculated values). R_8 stands for the R-state index of the atom number 8. q_{17} is the Wang-Ford charge of the atom number 17. *n*Cl is one constitutional descriptor. It stands for total number of chlorine atom of the molecule.

However, the final FA-MLR equation was developed with five descriptors. This is shown below in Eq. (6):

$$\begin{aligned}\mathrm{Log\ BA} &= -83.220(\pm 11.031) \\ &\quad +5.481(\pm 0.833)R_{16} - 8.075(\pm 1.362)q_{12} \\ &\quad -17.375(\pm 2.886)q_{19} + 34.953(\pm 4.943)Me \\ &\quad -1.469(\pm 0.172)I_1 \\ n &= 28;\ R = 0.907;\ R^2 = 0.822;\ R^2_{\mathrm{A}} = 0.782;\ F(5,22) \\ &= 20.337;\ p < 0.00001;\ \mathrm{S.E.E} = 0.140;\ R^2_{\mathrm{cv}} \\ &= 0.697;\ \mathrm{SSY} = 2.442;\ \mathrm{PRESS} = 0.740;\ \mathrm{SDEP} \\ &= 0.162;\ S_{\mathrm{PRESS}} = 0.83. \end{aligned} \quad (6)$$

R_{16} is the R-state index of the atom number 16. The positive coefficient associated with this parameter is indicative of the fact

Table 2
t-values and *p*-values of Eq. (2)–(6).

Eq. No	Intercept/Parameters	*t*-value	*p*-value
(2)	Intercept	41.129	0.000
	f_1	−2.794	0.010
	f_3	1.765	0.091
	f_4	−1.956	0.063
	f_7	−3.733	0.001
	f_8	−4.439	0.000
(4)	Intercept	−5.534	0.000
	R_{10}	−4.085	0.000
	R_{15}	6.132	0.000
	q_{14}	5.553	0.000
	q_{18}	5.313	0.000
(6)	$f^{(E)}5$	5.226	0.000
	Intercept	−7.544	0.000
	R_{16}	6.579	0.000
	q_{12}	−5.927	0.000
	q_{19}	−6.021	0.000
	Me	7.072	0.000
	I_1	−8.534	0.000
(3)	Intercept	−5.624	0.000
	S_{15}	−5.964	0.000
	R_{17}	4.610	0.000
	q_{12}	−5.327	0.000
	q_{14}	7.371	0.000
	q_{19}	−5.383	0.000
	$f^{(E)}5$	2.595	0.016
(5)	Intercept	6.995	0.000
	$S_{12/13}$	−6.665	0.000
	R_8	−3.709	0.001
	q_{17}	−5.610	0.000
	nCL	4.847	0.000
	$f^{(E)}5$	5.498	0.000

that the increase in the R-state index of this atom may be conducive to biological activity. *Me* is one constitutional descriptor. It stands for the mean atomic Sanderson electronegativity (scaled on carbon atom). Indicator parameter I_1 represents the presence or absence of methoxy group at R_1 position of the general structure.

The *t*-values and *p*-values of Eq. (3)–(6) are shown in Table 2. The correlation matrix of different descriptors used in the QSAR models is shown in Table 3. All models were validated by leave-one-out (LOO) cross-validation method. The observed (Obs), calculated (Calc.), residual (Res), predicted residual (PRES), and LOO-predicted activities of Eq. (2)–(6) are shown in Table 4a and b.

6. Discussion

The structure activity relationship of chemical structure with biological activity values suggested that the presence of methoxy group at R_1 position of the general structure may not be favorable for anticancer activity whereas the presence of chlorine substitution at R_2 position may be conducive to the biological activity.

Eq. (2) explains 61.6% and predicts 49.2% variances of the biological activity. The regression coefficients of variables f_3 and f_4 are significant at 91.0% and 94.0% levels respectively. These were supported by *t*- and *p*-values shown in Table 2. Eq. (2) shows importance of factor 1, 3, 4, 7 and 8. Factor loadings of different factors are included in Supplementary Material. Factor 1 was highly loaded with variables like S_{12}, S_{13}, S_{14}, S_{19}, S_{22}, R_{12}, R_{13}, R_{16}, R_{17}, R_{18}, R_{19}, R_{21}, R_{22}, *Ms*, *SA*(*G*), Vol, log*P*, *Refr*, *Pol*, *SIC*0, *IC*1, *SIC*1, *SIC*2 and *SIC*3. It showed importance of these parameters. Factor 3 was highly loaded with S_1, S_3, S_4, S_5, S_6, S_9, S_{10}, q_2, q_4 and *n*Cl. Factor 4 showed importance of parameters like R_1, R_2, R_3, R_4, R_5, R_6, R_9, R_{14} and *n*Br. Factor 7 was highly loaded with q_{18}, q_{19}, *IC*3, *IC*4 and *IC*5. Factor 8 was highly loaded with S_8, R_8, q_8, I_1 and $f^{(E)}5$. These factors showed the significance of these parameters.

Eq. (3) explains 77.0% and predicts 65.0% of variances of the biological activity. All regression coefficients involved in Eq. (3) are significant at 95% confidence level as suggested by *t*- and *p*-values shown in Table 2. The positive coefficient associated with the parameter $f^{(E)}5$ suggests that higher probability of electrophilic attack at the atom number 5 may be favorable to the biological activity. Negative coefficients of q_{12} and q_{19} indicate that increases in the negative charge or electron density at atom number 12 and 18 may be detrimental to the biological activity. The positive coefficient of q_{14} indicates that the increase in the negative charge or electron density at the atom number 14 may be favorable to higher antitumor activity. ETSA index is related with the electrostatic interaction. The negative coefficient associated with this parameter at the atom number 15 (S_{15}) indicates that the increase in the ETSA index of the atom number 15 may be detrimental to biological activity of these compounds. Refractotopological state atom index is assumed to be involved through the dispersive/van der Walls interactions. The positive coefficient of R_{17} in Eq. (3) indicates that the increase of the value of R-state index of the atom number 17 may improve antitumor activities of these molecules.

All regression coefficient of Eq. (4)–(6) are significant more than 95% confidence level. In Eq. (4), the negative coefficient of R_{10} suggests that the increase in the R-state index of the atom number 10 may be unfavorable for higher antitumor activity. The positive

Table 3
Correlation matrix of dependent and independent variables.

	BA	$S_{12/13}$	S_{15}	R_8	R_{10}	R_{15}	R_{16}	R_{17}	q_{12}	q_{14}	q_{17}	q_{18}	q_{19}	*Me*	*nCL*	I_1	$f^{(E)}5$
BA	1.00	−0.45	−0.19	0.33	−0.07	0.22	−0.20	−0.19	0.19	0.45	0.02	0.04	−0.32	0.31	0.44	−0.49	0.47
$S_{12/13}$		1.00	0.14	−0.53	0.18	−0.22	0.89	0.90	0.09	−0.60	−0.57	0.40	−0.11	−0.69	−0.06	0.60	−0.17
S_{15}			1.00	0.03	0.15	−0.55	−0.06	0.00	−0.40	0.31	−0.24	0.42	0.18	−0.56	−0.15	−0.18	−0.07
R_8				1.00	−0.42	−0.28	−0.59	−0.55	0.32	0.68	0.12	−0.25	0.04	0.38	0.33	−0.77	0.36
R_{10}					1.00	0.44	0.37	0.33	−0.37	−0.32	−0.24	0.45	−0.15	−0.47	−0.49	0.41	0.05
R_{15}						1.00	0.15	0.07	−0.02	−0.26	0.15	−0.16	−0.08	0.42	0.02	0.41	−0.10
R_{16}							1.00	0.99	0.21	−0.58	−0.59	0.35	−0.18	−0.59	−0.03	0.60	−0.11
R_{17}								1.00	0.24	−0.53	−0.62	0.35	−0.17	−0.63	−0.03	0.54	−0.10
q_{12}									1.00	0.29	−0.28	−0.42	−0.21	0.21	0.25	−0.30	0.11
q_{14}										1.00	0.05	−0.36	0.23	0.30	0.22	−0.85	0.19
q_{17}											1.00	−0.53	0.28	0.49	0.13	−0.18	0.31
q_{18}												1.00	−0.57	−0.64	−0.11	0.28	−0.11
q_{19}													1.00	0.11	−0.10	−0.14	−0.10
Me														1.00	0.31	−0.20	−0.06
nCL															1.00	−0.24	0.21
I_1																1.00	−0.39
$f^{(E)}5$																	1.00

Table 4a
Observed (Obs), calculated (Calc), residual (Res), predicted residual (Pres) and LOO-predicted (Pred) activities of Eq. (2)–(4).

Cpd	Obs	Eq. (2)				Eq. (3)				Eq. (4)			
		Calc	Res	Pres	Pred	Calc	Res	Pres	Pred	Calc	Res	Pres	Pred
18	1.584	1.737	−0.153	−0.209	1.793	1.619	−0.035	−0.045	1.629	1.584	0.000	0.000	1.584
19	1.841	1.839	0.002	0.002	1.838	1.862	−0.021	−0.030	1.871	1.638	0.203	0.223	1.618
20	1.446	1.404	0.042	0.047	1.399	1.575	−0.129	−0.147	1.593	1.446	−0.001	−0.001	1.446
21	1.153	1.296	−0.143	−0.155	1.308	1.370	−0.218	−0.242	1.394	1.234	−0.082	−0.092	1.245
22	1.209	1.558	0.085	0.102	1.541	1.669	−0.026	−0.033	1.676	1.631	0.012	0.015	1.628
23	1.643	1.312	−0.104	−0.113	1.322	1.212	−0.003	−0.004	1.213	1.209	0.000	0.000	1.209
24	1.792	1.982	−0.190	−0.292	2.084	1.683	0.109	0.159	1.634	1.612	0.180	0.233	1.559
25	1.246	1.357	−0.110	−0.124	1.370	1.209	0.037	0.048	1.198	1.246	0.000	0.000	1.246
26	1.730	1.593	0.138	0.176	1.555	1.332	0.399	0.444	1.287	1.500	0.230	0.306	1.424
27	1.537	1.627	−0.090	−0.116	1.654	1.502	0.036	0.039	1.498	1.657	−0.120	−0.158	1.696
28	1.686	1.766	−0.080	−0.123	1.809	1.681	0.005	0.006	1.680	1.808	−0.122	−0.158	1.844
29	1.668	1.757	−0.089	−0.108	1.775	1.869	−0.201	−0.264	1.931	1.436	0.232	0.259	1.409
30	1.687	1.488	0.200	0.215	1.472	1.639	0.048	0.053	1.635	1.743	−0.056	−0.068	1.755
31	1.595	1.397	0.198	0.212	1.383	1.570	0.025	0.027	1.568	1.532	0.063	0.068	1.527
32	1.876	1.665	0.211	0.239	1.638	1.844	0.032	0.048	1.828	1.906	−0.030	−0.036	1.913
33	1.616	1.463	0.057	0.063	1.457	1.425	0.095	0.102	1.418	1.520	0.000	0.000	1.520
34	1.703	1.675	−0.059	−0.087	1.703	1.582	0.034	0.037	1.578	1.695	−0.079	−0.113	1.728
35	1.361	1.576	0.127	0.147	1.557	1.742	−0.039	−0.050	1.753	1.910	−0.207	−0.282	1.986
36	1.520	1.423	−0.062	−0.114	1.475	1.469	−0.108	−0.120	1.481	1.408	−0.047	−0.087	1.447
37	1.765	1.567	0.198	0.294	1.471	1.527	0.239	0.287	1.479	1.632	0.134	0.173	1.592
38	1.026	0.983	0.043	0.354	0.672	1.028	−0.002	−0.012	1.038	1.325	−0.299	−0.344	1.370
39	1.210	1.211	−0.001	−0.001	1.212	1.365	−0.155	−0.174	1.384	1.159	0.051	0.060	1.150
40	1.172	1.093	0.079	0.096	1.076	1.219	−0.047	−0.056	1.228	1.265	−0.093	−0.103	1.275
41	1.018	1.261	−0.243	−0.274	1.292	1.121	−0.103	−0.145	1.163	1.018	0.000	0.000	1.018
42	1.371	1.286	0.085	0.149	1.222	1.221	0.150	0.179	1.193	1.343	0.028	0.047	1.324
43	1.274	1.314	−0.040	−0.087	1.361	1.076	0.198	0.290	0.984	1.133	0.141	0.287	0.986
44	0.637	0.765	−0.127	−0.224	0.861	0.859	−0.221	−0.344	0.981	0.777	−0.140	−0.244	0.881
45	1.170	1.143	0.027	0.045	1.125	1.266	−0.096	−0.144	1.314	1.171	−0.001	−0.002	1.172

coefficient of R_{15} indicates that the increase in the R-state index of the atom number 15 may be favorable for the biological activity. The positive coefficient associated with q_{18} suggested that with the increase in the positive charge of the atom number 18 may be conducive to the biological activity of these glutamamide compounds. This means that electron density of this atom may be needed to be decreased for higher biological activity. Eq. (4) explains 73.8% and predicts 67.0% of variances of the biological activity.

Eq. (5) explains 74.6% and predicts 60.7% of variances of the biological activity. The negative coefficient associated with $S_{12/13}$ indicates that the increase in the E-state index of the atom number 12 as well as that of 13 may be detrimental to the biological activity. The negative coefficient of R_8 suggests that the increase in the R-state

Table 4b
Observed (Obs), calculated (Calc), residual (Res), predicted residual (Pres) and LOO-predicted (Pred) activities of Eq. (5)–(6).

Cpd	Obs	Eq. (5)				Eq. (6)			
		Calc	Res	Pres	Pred	Calc	Res	Pres	Pred
18	1.584	1.651	−0.067	−0.088	1.671	1.718	−0.134	−0.176	1.759
19	1.841	1.733	0.108	0.128	1.713	1.675	0.166	0.209	1.632
20	1.446	1.595	−0.149	−0.166	1.612	1.591	−0.145	−0.167	1.613
21	1.153	1.335	−0.182	−0.197	1.349	1.444	−0.292	−0.320	1.473
22	1.209	1.267	−0.058	−0.063	1.272	1.391	−0.182	−0.202	1.411
23	1.643	1.658	−0.015	−0.017	1.660	1.732	−0.089	−0.112	1.755
24	1.792	1.856	−0.064	−0.119	1.911	1.703	0.089	0.117	1.675
25	1.246	1.287	−0.040	−0.046	1.292	1.337	−0.090	−0.125	1.372
26	1.730	1.631	0.099	0.203	1.528	1.283	0.448	0.536	1.195
27	1.537	1.278	0.259	0.308	1.229	1.447	0.090	0.108	1.429
28	1.686	1.744	−0.058	−0.079	1.765	1.717	−0.031	−0.046	1.732
29	1.668	1.809	−0.142	−0.168	1.835	1.596	0.071	0.086	1.582
30	1.687	1.668	0.020	0.022	1.665	1.578	0.109	0.126	1.561
31	1.595	1.639	−0.045	−0.050	1.645	1.542	0.052	0.059	1.535
32	1.876	1.839	0.037	0.045	1.832	1.886	−0.010	−0.015	1.891
33	1.616	1.491	0.125	0.144	1.472	1.722	−0.107	−0.137	1.752
34	1.703	1.415	0.288	0.356	1.348	1.639	0.065	0.077	1.626
35	1.361	1.600	−0.239	−0.299	1.660	1.554	−0.193	−0.242	1.602
36	1.520	1.507	0.013	0.015	1.505	1.473	0.047	0.055	1.465
37	1.765	1.459	0.306	0.394	1.372	1.445	0.320	0.414	1.352
38	1.026	0.963	0.063	0.625	0.401	1.225	−0.199	−0.268	1.294
39	1.210	1.283	−0.073	−0.081	1.291	1.210	0.000	0.000	1.210
40	1.172	1.208	−0.036	−0.041	1.213	1.155	0.017	0.020	1.152
41	1.018	1.117	−0.099	−0.119	1.137	1.074	−0.056	−0.077	1.095
42	1.371	1.282	0.089	0.106	1.265	1.256	0.115	0.153	1.218
43	1.274	1.216	0.058	0.078	1.195	1.046	0.228	0.353	0.920
44	0.637	0.836	−0.198	−0.308	0.945	0.876	−0.238	−0.367	1.004
45	1.170	1.169	0.001	0.001	1.169	1.221	−0.051	−0.079	1.249

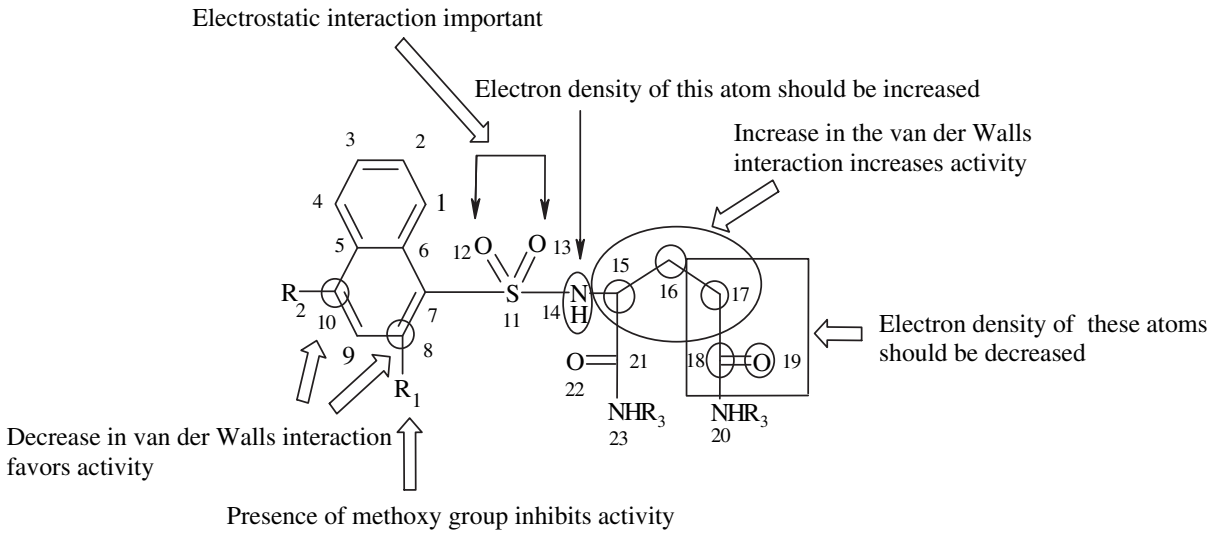

Fig. 4. Important atoms and substitution of 1, 5-*N*,*N*′-substituted-2-(substituted naphthalenesulphonyl) glutamamides.

index of the atom number 8 may not be favorable for anticancer activity of these compounds. The negative coefficient of q_{17} indicates that higher biological activity may correspond to decrease in the negative charge or electron density of the atom number 17. *n*Cl is one constitutional descriptor. It stands for total number of chlorine atom of the molecule. The positive coefficient associated with this descriptor indicates that increase in the total number of chlorine atom of these molecules may be favorable to the biological activity.

Eq. (6) explains 78.2% and predicts 69.7% of variances of the biological activity. R_{16} is the R-state index of the atom number 16. The positive coefficient associated with this parameter is indicative of the fact that with the increase in the R-state index of this atom may be conducive to the biological activity. The positive coefficient of *Me* indicates that the increase in the mean atomic electronegativity of these compounds may correspond to higher biological activity. Indicator parameter I_1 stands for presence or absence of methoxy group at R_1 position of the general structure. The negative coefficient of this parameter suggests that the presence of this group at R_1 position may be unfavorable for biological activity.

7. Conclusion

From the study, it is evident that these twenty eight synthesized glutamamide analogs have varying anticancer activities. Comparative QSAR study showed that the decrease in the electrostatic interactions of atom number 12/13 and 15 may be conducive to antitumor activity of these compounds. Decreases in the R-state indices of atom numbers 8 and 10 and increase in the R-state indices of the atom numbers 15, 16 and 17 may be favorable to the biological activity. The increase in the charges of atom numbers 14 and 18 as well as the decrease in the charges of atom numbers 12, 17 and 19 may be conducive to higher biological activity. From the calculated charges of these atoms, it is obvious that electron density may be decreased in atom numbers 12, 17, 18 and 19 whereas electron density may be increased in the atom number 14. QSAR study also revealed the fact that the presence of methoxy group at R_1 position may be unfavorable for higher antitumor activity of these glutamamides. The increase in the number of chlorine atom in the molecule as well as mean atomic electronegativity of these compounds may lead to higher anticancer activity. QSAR study emphasizes that higher probability of electrophilic attack at the atom number 5 may be favorable to the biological activity. QSAR results are shown diagramically in Fig. 4. The current study allows us to investigate the structural features of these synthesized glutamamide compounds. It may help in further tailoring of these analogs to get an active member.

8. Experimental

8.1. Chemistry

All reactions were monitored by analytical thin layer chromatography performed on silica gel G plates. Spots were located keeping these TLC plates in iodine chamber. Final compounds were obtained as solid crystalline forms. Structures of these synthesized compounds were confirmed by IR, ^{1}H NMR, mass spectra and elemental analyses. Melting points of all synthesized compounds were first measured on Mel-Temp, a capillary melting point apparatus. These were verified in CTRONICS, a digital melting point apparatus. Infrared spectra were recorded on SASCO FTIR-410 Model Fourier Transformed Infrared spectrophotometer of SHIMADZU using KBr pellets. Running the spectrum of 0.05 mm polystyrene film did the finer calibration of the machine. Frequencies were expressed in cm^{-1}. Proton Nuclear Magnetic Resonance (^{1}H NMR) spectra were collected at 25 °C in the pulsed Fourier Transformation mode on Bruker DPX 300 MHz spectrophotometers. Chemical shifts are reported in δ ppm (parts per million) relative to Tetramethyl Silane (Me_4Si) as an internal standard for solutions in deuteriorated chloroform ($CDCl_3$). Splitting patterns have been designated as s (singlet), d (doublet), t (triplet), dd (doublet of doublet) and m (multiplet). Positions of the hydrogen atoms described in ^{1}H NMR interpretation are as per general structure (Fig. 1). Substitutions at the R_3 position has taken the superscript ‘″’ (double dash) and the substitution at R_3' position has taken the superscript ‘‴’ (triple dash). The mass spectra (FAB/

Table 5
Physical data of the intermediate compounds.

Cpd	R_1	R_2	mp (°C)	% Yield	Molecular formula	M_w
5	H	H	63–65	72.92	$C_{10}H_7ClO_2S$	226.67
6	H	Cl	78–80	96.13	$C_{10}H_6Cl_2O_2S$	261.12
7	H	Br	82–84	74.53	$C_{10}H_6ClBrO_2S$	305.57
8	OCH_3	H	110–112	11.13	$C_{11}H_9ClO_3S$	256.70
10	H	H	96–98	78.69	$C_{15}H_{15}NO_6S$	337.38
11	H	Cl	180–182	78.38	$C_{15}H_{14}ClNO_6S$	371.82
12	H	Br	154–156	69.45	$C_{15}H_{14}BrNO_6S$	416.28
13	OCH_3	H	170–172	42.31	$C_{16}H_{17}NO_7S$	367.41

Table 6
Physical data of synthesized 1,5-*N*,*N*′-disustituted-2-(substituted naphthalenesulphonyl) glutamamides (**18–45**).

Cpd.[a] No.	R_1	R_2	R_3/R_3'	M_w	% Yield	Structural formula	mp (°C)
18	H	H	H	335.39	19.43	$C_{15}H_{17}N_3O_4S$	165–167
19	H	H	CH_3	363.48	74.52	$C_{17}H_{21}N_3O_4S$	184–186
20	H	H	C_2H_5	391.54	80.23	$C_{19}H_{25}N_3O_4S$	120–122
21	H	H	*n*-C_3H_7	419.60	59.36	$C_{21}H_{29}N_3O_4S$	153–154
22	H	H	*i*-C_3H_7	419.60	60.25	$C_{21}H_{29}N_3O_4S$	170–172
23	H	H	*n*-C_4H_9	447.66	53.44	$C_{23}H_{33}N_3O_4S$	152–154
24	H	H	*i*-C_4H_9	447.66	77.23	$C_{23}H_{33}N_3O_4S$	158–160
25	H	H	*n*-C_5H_{11}	474.84	68.66	$C_{25}H_{37}N_3O_4S$	114–116
26	H	H	C_6H_{11}	499.39	60.80	$C_{27}H_{37}N_3O_4S$	226–228
27	H	H	$C_6H_5CH_2$	515.68	73.55	$C_{29}H_{29}N_3O_4S$	156–158
28	H	Cl	H	369.86	69.36	$C_{15}H_{16}N_3O_4SCl$	227–229
29	H	Cl	CH_3	397.92	42.63	$C_{17}H_{20}N_3O_4SCl$	235–237
30	H	Cl	C_2H_5	425.96	48.96	$C_{19}H_{24}N_3O_4SCl$	201–203
31	H	Cl	*n*-C_3H_7	454.04	50.20	$C_{21}H_{28}N_3O_4SCl$	183–185
32	H	Cl	*i*-C_3H_7	454.04	36.24	$C_{21}H_{28}N_3O_4SCl$	167–167
33	H	Cl	*n*-C_4H_9	482.10	62.99	$C_{23}H_{32}N_3O_4SCl$	148–150
34	H	Cl	*i*-C_4H_9	482.10	33.62	$C_{23}H_{32}N_3O_4SCl$	192–194
35	H	Cl	C_6H_{13}	537.62	51.90	$C_{27}H_{40}N_3O_4SCl$	156–158
36	H	Cl	$C_6H_5CH_2$	549.36	64.28	$C_{29}H_{28}N_3O_4SCl$	181–183
37	H	Br	H	414.31	67.84	$C_{15}H_{16}N_3O_4SBr$	217–219
38	H	Br	CH_3	442.37	55.56	$C_{17}H_{20}N_3O_4SBr$	241–243
39	H	Br	C_2H_5	470.43	60.52	$C_{19}H_{24}N_3O_4SBr$	211–213
40	H	Br	*n*-C_3H_7	498.44	71.23	$C_{21}H_{28}N_3O_4SBr$	186–188
41	H	Br	*n*-C_5H_{11}	554.56	57.73	$C_{25}H_{36}N_3O_4SBr$	158–160
42	H	Br	$C_6H_5CH_2$	594.57	55.25	$C_{29}H_{28}N_3O_4SBr$	180–182
43	OCH_3	H	$C_6H_5CH_2$	545.71	27.56	$C_{30}H_{31}N_3O_5S$	160–162
44	OCH_3	H	C_6H_{11}	529.70	33.65	$C_{28}H_{39}N_3O_5S$	169–171
45	OCH_3	H	C_6H_{13}	533.73	42.43	$C_{28}H_{43}N_3O_5S$	178–180

[a] Cpd = Compound.

EI) were recorded on API 200 mass spectrophotometer. Elemental analyses or microanalyses (C, H, N) of these compounds were performed on 2400 Series-II CHN analyzer of Perkin–Elmer. The general structures of starting materials, intermediates as well as the synthetic scheme are given in Fig. 2. Physical data of intermediate compounds are shown in Table 5. Physical data and spectral data of all final compounds are given in Tables 6 and 7 respectively.

8.2. Anticancer activity

Swiss albino mice of either sex (female in this case) of 10 weeks old with an average body weight of 18–20 g were used for *in vivo* method. All mice were kept on basal metabolic diet with water *ad libitum*. The ambient room temperature (25–27 °C) was maintained during these experiments. Two groups of Swiss Albino mice were made. Each group was containing six healthy female mice. These were having approximately of the same age and body weight (18–20 g). Animals were selected at random. One of these two groups was served as the control while the other was served as the test. Ehrlich Ascites Carcinoma (EAC) cells were collected from the donor mouse. These were suspended in sterile isotonic solution (0.9% w/v NaCl). Numbers of tumor cells per ml of this suspension were counted under microscope with the help of a haemocytometer manufactured by Marienfeld, Germany. About 2×10^6 cells/0.2 mL of these living viable cells were injected into the peritoneal cavity of each mouse. In this instance, tumor cells multiplied relatively freely within the peritoneal cavity. Ascites were developed in the cavity. A day of incubation was allowed to establish the disease in the body before starting the administration of the drug. From the second day of transplantation up to the eighth day, a suitable challenge dose (0.2 m mol/kg body weight) of the drug solution/suspension in sterile phosphate buffer (pH 7.2) were injected intraperitoneally to each mouse in the test group at 24 h interval. Thus, seven doses of the compound and standard drug were administered intraperitoneally from the first day of injection up to the seventh day with 24 h intervals to each mouse in the test group. Control animals received only the vehicle. On the ninth day, food and water was withheld 6 h before sacrificing these animals. Weights of all the animals were recorded before these were sacrificed. The peritoneal cavity was dissected. The ascitic fluid was withdrawn by a syringe to a suitable volume. It was collected in sterile ice cold saline. This was preserved in ice bath. The number of living cells/ml in the peritoneal fluid of each mouse in a group were counted using trypan blue as an indicator. These were done under a microscope with the help of a haemocytometer. After removing the fluid from the peritoneal cavity for cell count, ascitic fluid was wiped off with absorbent cotton. The weight of the six mice after sacrifice was recorded. The difference in weight was considered as the tumor weight.

The mean of Ascites cells/ml was taken for evaluation of antineoplastic activity. The evaluation of the test drug was made by comparing the cell count and tumor weight of the test with that of the control.

8.3. QSAR study

Topological descriptors like electrotopological state atom index (ETSA) [30–35] and refractotopological state atom index (RTSA) [36–39] were calculated by using the computer program 'Mouse' [40] developed in our laboratory. Calculation of different quantum chemical descriptors like approximate molecular surface area [*SA*(*A*)], molecular surface area grid [*SA*(*G*)], hydrophobicity (log*P*), molecular volume (Vol), molecular polarizability (*Pol*), molecular refractivity (*Refr*), hydration energy (HE) and frontier electron density electrophilic ($f^{(E)}$) were done using the computer program Hyperchem Release 7.0 Pro. Package [41]. In Hyperchem software, the 2D structures of these compounds were drawn. These were converted to corresponding 3D structures. Energy minimization of these structures were done using molecular mechanical (MM+) force fields without cut-off for non-bonded interactions, solvation and constrains. These energy minimized structures were subjected to geometrical optimization by semi-empirical AM1 (Austin model 1) method using Polak-Ribiere algorithm with an RMS gradient of

Table 7
Mass, IR, prton NMR and CHN analysis data of the final compounds (**18**–**45**).

Cpd	Mass (FAB)	IR (KBr, cm^{-1})	^1H NMR (300MHz, $CDCl_3$))	C, H, N % calcd/found		
				C	H	N
18	$M + H^+$ peak at *m/z* 336	3481 (Asymmetric N–H str. of $CONH_2$), 3376 (Symmetric N–H str. of $CONH_2$), 3146 (Ar C–H str.), 2861 (ali C–H str.), 1666 (C═O str. of $CONH_2$), 1426 (Ar–C═CH str.), 1311 (S═O str of SO_2NH, asymmetric), 1158 (S═O str. of SO_2NH, symmetric), 798, 767, 684 (Polynuclear-CH out of plane bending)	δ 8.73 (s, 1H, SO_2NH), δ 7.32–8.23 (m, 7H, H-2′, H-3′, H-4′, H-6′, H-7′, H-8′, H-9′), δ 5.85 (m, 2H, $CONH_2$-1), δ 5.34 (m, 2H, $CONH_2$-5), δ 3.67 (m, 1H, H-2), δ 2.27 (m, 2H, H_2-4), δ 2.01 (m, 2H, H_2-3), 1.78 (m, 1H, H_B-3)	53.57/53.96	5.06/4.96	12.50/12.68
19	$M + H^+$ peak at *m/z* 364	3315 (NH str. Of CONH), 3107 (Ar. CH Str), 2933 ali C–H str.), 1647 (C═O str. of COOH), 1556 (NH bend of CONH), 1458,1436, 1413 (Ar. C═CH str), 1357 (S═O str. of SO_2NH, asymmetric), 1161 (S═O str. of SO_2NH, symmetric), 802, 767, 680 (Polynuclear-CH out of plane bending)	δ 8.73 (s, 1H, SO_2NH), δ 7.50–8.23 (m, 7H, H-2′, H-3′, H-4′, H-6′, H-7′, H-8′, H-9′), δ 6.71 (m, 1H, CONH-1), δ 5.61 (m, 1H, CONH-5), δ 3.61 (m, 1H, H-2), δ 2.72 (m, 3H, N–CH_3-1‴), δ 2.52 (m, 3H, N–CH_3-1″), δ 2.17 (m, 2H, H_2-4), δ 1.87 (m, 2H, H_2-3)	56.14/56.74	5.77/5.45	11.55/11.63
20	$M + H^+$ peak at *m/z* 392	3301 (N–H str of CONH), 3091 (Ar C–H str.), 2958, 2871 (ali C–H str.), 1643 (C═O str. of CONH), 1556 (N–H bend of CONH), 1508, 1438 (Ar C═CH str), 1317 (S═O str of SO_2NH, asymmetric), 1154 (S═O str of SO_2NH, symmetric), 802, 767, 680 (Polynuclear-CH out of plane bending)	δ 8.76 (s, 1H, SO_2NH), δ 7.68–8.40 (m, 6H, H-2′, H-3′, H-4′, H-6′, H-7′, H-8′, H-9′), δ 6.58 (m, 1H, CONH-1), δ 5.51 (m, 1H, CONH-5), δ 3.62 (m, 1H, H-2), δ 3.24 (m, 2H, NH–CH_2-1″), δ 2.96 (m, 2H, NH–CH_2-1‴), 2.23 (m, 2H, H_2-4), δ 2.02 (m, 1H, H_A-3), δ 1.77 (m, 1H, H_B-3), 1.11–1.63 (m, 1H, CH_3-2″) δ 0.80–1.11 (m, 3H, CH_3-2‴)	58.23/58.93	6.38/6.12	10.73/10.82
21	$M + H^+$ peak at *m/z* 420	3294 (N–H str of CONH), 3101 (Ar C–H str.), 2960, 2871 (ali C–H str.), 1645 (C═O str. of CONH), 1558(N–H bend of CONH), 1436 (Ar C═CH str), 1319 (S═O str of SO_2NH, asymmetric), 1155 (S═O str of SO_2NH, symmetric), 800, 767, 680 (Polynuclear-CH out of plane bending)	δ 8.75 (s, 1H, SO_2NH), δ 7.49–8.23 (m, 7H, H-2′, H-3′, H-4′, H-6′, H-7′, H-8′, H-9′), δ 6.61 (m, 1H, CONH-1), δ 5.53 (m, 1H, CONH-5), δ 3.60 (m, 1H, H-2), δ 3.16–3.20(m, 2H, N–CH_2-1″,), δ 2.83–2.95 (m, 2H, N–CH_2-1‴), δ 2.23 (m, 2H, H_2-4), δ 2.04 (m, 1H, H_A-3), δ 1.78 (m, 1H, H_B-3), δ 1.45–1.55 (m, 2H, N–CH_2-2″), δ 1.24–1.12 (m, 2H, N–CH_2-2‴), δ 0.96–0.91 (m, 3H, 3H, N–CH_2-3″), δ 0.68–0.73 (m, 3H, 3H, N–CH_2-3‴)	60.14/59.89	6.92/6.93	10.02/9.17
22	$M + H^+$ peak at *m/z* 420	3295 (N–H str of CONH), 3079 (Ar C–H str.), 2973 (ali C–H str.), 1643(C═O str. of CONH), 1550(N–H bend of CONH), 1454(Ar–C═CH str), 1329(S═O str of SO_2NH, asymmetric), 1154 (S═O str of SO_2NH, symmetric), 909, 836, 681 (Polynuclear-CH out of plane bending)	8.78 (s, 1H, SO_2NH), δ 7.61–8.43 (m, 7H, H-2′, H-3′, H-4′, H-6′, H-7′, H-8′, H-9′), δ 6.35 (m, 1H, CONH-1), δ 5.50 (m, 1H, CONH-5), δ 4.01 (m, 2H, N–CH-1″, N–CH-1‴), δ 3.64 (m, 1H, H-2), δ 2.23 (m, 2H, H_2-4), δ 2.04 (m, 1H, H_A-3), δ 1.78 (m, 1H, H_B-3), δ 1.24–1.14 (m, 6H, CH_3-2″, CH_3-2‴), δ 0.83–0.75 (m, 6H, CH_3-4″, CH_3-4‴)	60.14/59.34	6.92/6.95	10.02/9.18
23	$M + H^+$ peak at *m/z* 448	3309 (N–H str of CONH), 3087 (Ar C–H str.), 2977, 2935 (ali C–H str.), 1642 (C═O str. of CONH), 1552(N–H bend of CONH), 1436 (Ar C═CH str), 1323 (S═O str of SO_2NH, asymmetric), 1159 (S═O str of SO_2NH, symmetric), 803, 768, 678 (Polynuclear-CH out of plane bending)	δ 8.77 (s, 1H, SO_2NH), δ 7.49–8.21 (m, 7H, H-2′, H-3′, H-4′, H-6′, H-7′, H-8′, H-9′), δ 5.58 (m, 1H, CONH-1), δ 5.34 (m, 1H, CONH-5), δ 3.67 (m, 1H, H-2), δ 3.28–3.30(m, 2H, N–CH_2-1″,), δ 2.90–2.96 (m, 2H, N–CH_2-1‴), δ 2.32 (m, 2H, H_2-4), 2.12–2.17 δ (m, 4H, N–CH_2-2″, N–CH_2-2‴), δ 2.07 (m, 1H, H_A-3), δ 1.89–1.90 (m, 4H, N–CH_2-3″, N–CH_2-3‴), δ 1.13–1.18 (m, 3H, N–CH_3-4″), δ 0.73–0.78 (m, 3H, N–CH_3-4‴)	61.65/61.87	7.37/7.14	9.38/9.35
24	$M + H^+$ peak at *m/z* 448	3302(N–H str of CONH), 3095 (Ar C–H str.), 2959 (ali C–H str.), 1647 (C═O str. of CONH), 1555 (N–H bend of CONH), 1444 (Ar–C═CH str), 1322 (S═O str of SO_2NH, asymmetric), 1159 (S═O str of SO_2NH, symmetric), 770, 680 (Polynuclear-CH out of plane bending)	δ 8.76 (s, 1H, SO_2NH), δ 7.61–8.46 (m, 6H, H-2′, H-3′, H-4′, H-6′, H-7′, H-8′, H-9′), δ 6.70 (m, 1H, CONH-1), δ 5.56 (m, 1H, CONH-5), δ 3.63 (m, 1H, H-2), 3.01 (m, 2H, NH–CH_2-1″), δ 2.76 (m, 2H, NH–CH_2-1‴), δ 2.29 (m, 2H, H_2-4), δ 2.04 (m, 1H, H_A-3), δ 1.86 (m, 1H, H_B-3), δ 1.70–1.86 (m, 2H, NH–CH_2–CH-2″, NH–CH_2–CH-2‴), δ 0.90–0.93 (d, 6H, CH_3-4″, CH_3-4‴), δ 0.70–0.74 (d, 2H, CH_3-3″, CH_3-3‴)	61.65/61.54	7.37/7.15	9.38/9.39
25	$M + H^+$ peak at *m/z* 475	3301 (N–H str of CONH), 3091 (Ar C–H str.), 2958, 2871 (ali C–H str.), 1643 (C═O str. of CONH), 1556 (N–H bend of CONH), 1508, 1438 (Ar C═CH str), 1317 (S═O str of SO_2NH, asymmetric), 1154 (S═O str of SO_2NH, symmetric), 802, 767, 680 (Polynuclear-CH out of plane bending.	δ 8.73 (s, 1H, SO_2NH), δ 7.32–8.23 (m, 7H, H-2′, H-3′, H-4′, H-6′, H-7′, H-8′, H-9′), δ 5.85 (m, 1H, $CONH_2$-1), δ 5.34 (m, 1H, CONH-5), δ 3.67 (m, 1H, H-2), δ3.68 (m, 2H, N–CH_2-1″), δ 3.13 (m, 2H, N–CH_2-1″), δ 2.27 (m, 2H, H_2-4), δ 2.01 (m, 2H, H_2-3), δ 1.78 (m, 1H, H_B-3), δ1.56–1.29 (m, 12H, CH_2-2″, CH_2-3″, CH_2-4″, CH_2-2‴, CH_2-3‴, CH_2-4‴), δ 0.97–0.74 (m, 6H, CH_3-5″, CH_3-5‴)	63.18/63.42	7.79/7.56	8.84/8.96
26	$M + H^+$ peak at *m/z* 499	3286 (N–H str of CONH), 3086(Ar C–H str.), 2929 (ali C–H str.), 1643(C═O str. of CONH), 1551 (N–H bend of CONH), 1445 (Ar–C═C), 1320 (S═O str of SO_2NH, asymmetric), 1154 (S═O str of SO_2NH, symmetric), 893, 805, 771 (Polynuclear-CH out of plane bending)	δ 8.73 (s, 1H, SO_2NH), δ 7.48–8.22 (m, 6H, H-2′, H-3′, H-4′, H-6′, H-7′, H-8′, H-9′), δ 6.35 (m, 1H, CONH-1), δ 5.44 (m, 1H, CONH-5), δ 3.36 (m, 1H, H-2), δ 2.23 (m, 2H, H_2-4), δ 2.02–2.09 (m, 2H, H_2-3), δ 1.01–1.90 (m, 22H, Cyclohexyl protons)	64.92/64.56	7.21/7.12	8.41/8.63
27	$M + H^+$ peak at *m/z* 516	3293 (N–H str. of CONH), 3083 (Ar C–H str.), 2929 (ali C–H str.), 1647 (C═O str. of CONH), 1550 (N–H bend of CONH), 1442 (Ar C═CH str.), 1323 (S═O str. of SO_2NH, asymmetric), 1150 (S═O str. of SO_2NH, symmetric), 887, 834, 757, 680 (Polynuclear and mononuclear Ar.–CH out of plane bending);	8.72 (s, 1H, SO_2NH), δ 7.29–8.35 (m, 19H, H-2′, H-3′, H-4′, H-6′, H-7′, H-8′, H-9′, H-2″, H-3″, H-5″, H-6″, H-7″, H-8″, H-2‴, H-3‴, H-5‴, H-6‴, H-7‴, H-8‴), δ 6.93 (m, 1H, CONH-1), δ 5.82 (m, 1H, CONH-5), δ 4.04–4.41 (m, 4H, NH–CH_2-1″, NH–CH_2-1‴), δ 3.70 (m, 1H, H-2), 2.29 (m, 2H, H_2-4), δ 2.03 (m, 1H, H_A-3), δ 1.77–1.84 (m, 1H, H_B-3)	67.44/67.67	5.62/5.45	8.14/8.23

28	$M + H^+$ peak at m/z 370	3480 (Asymmetric N–H str. of $CONH_2$), 3336 (Symmetric N–H str. of $CONH_2$), 3172 (Ar C–H str.), 2863 (ali C–H str.), 1664 (C═O str. of $CONH_2$), 1424 (Ar–C═CH str.), 1312 (S═O str of SO_2NH, asymmetric), 1136 (S═O str. of SO_2NH, symmetric), 831, 759, 683 (Polynuclear-CH out of plane bending)	δ 8.73 (s, 1H, SO_2NH), δ 7.32–8.23 (m, 6H, H-2′, H-3′, H-6′, H-7′, H-8′, H-9′), δ 5.85 (m, 2H, $CONH_2$-1), δ 5.34 (m, 2H, $CONH_2$-5), δ 3.67 (m, 1H, H-2), δ 2.27 (m, 2H, H_2-4), δ 2.01 (m, 2H, H_2-3), 1.78 (m, 1H, H_B-3).	48.71/48.10	4.32/4.11	11.35/11.29
29	$M + H^+$ peak at m/z 398	3304, 3262 (N–H str. of CONH), 3109 (Ar C–H str.), 2943 (ali C–H str.), 1644 (C═O str. of CONH), 1567(N–H bend of CONH), 1504, 1441 (Ar–C═CH str.), 1318 (S═O str of SO_2NH, asymmetric), 1146 (S═O str of SO_2NH, symmetric), 916, 834, 756, 688 (Polynuclear-CH out of plane bending)	δ 8.73 (s, 1H, SO_2NH), δ 7.50–8.23 (m, 6H, H-2′, H-3′, H-6′, H-7′, H-8′, H-9′), δ 6.71 (m, 1H, CONH-1), δ 5.61 (m, 1H, CONH-5), δ 3.61 (m, 1H, H-2), δ 2.72 (m, 3H, N–CH_3-1‴), δ 2.52 (m, 3H, N–CH_3-1″), δ 2.17 (m, 2H, H_2-4), δ 1.87 (m, 2H, H_2-3)	51.26/51.01	4.77/4.78	10.55/10.43
30	$M + H^+$ peak at m/z 426	3301 (N–H str of CONH), 3091 (Ar C–H str.), 2958, 2871 (ali C–H str.), 1643 (C═O str. of CONH), 1556 (N–H bend of CONH), 1508, 1438 (Ar C═CH str), 1317 (S═O str of SO_2NH, asymmetric), 1154 (S═O str of SO_2NH, symmetric), 1043 (Ar–Cl), 802, 767, 680 (Polynuclear-CH out of plane bending).	δ 8.76 (s, 1H, SO_2NH), δ 7.68–8.40 (m, 6H, H-2′, H-3′, H-6′, H-7′, H-8′, H-9′), δ 6.58 (m, 1H, CONH-1), δ 5.51 (m, 1H, CONH-5), δ 3.62 (m, 1H, H-2), δ 3.24 (m, 2H, NH–CH_2-1″), δ 2.90 (m, 2H, NH–CH_2-1‴), 2.23 (m, 2H, H_2-4), δ 2.02 (m, 1H, H_A-3), δ 1.77 (m, 1H, H_B-3), 1.11–1.63 (m, 3H, CH_3-2″) δ 0.80–1.11 (m, 3H, CH_3-2‴)	53.52/53.56	5.40/5.76	9.86/9.56
31	$M + H^+$ peak at m/z 454	3297 (N–H str. of CONH), 3092 (Ar C–H str.), 2961(ali C–H str.), 1647 (C═O str. of CONH), 1556 (N–H bend of CONH), 1438 (Ar C═CH str.) 1328 (S═O str. of SO_2NH, asymmetric), 1154 (S═O str. of SO_2NH, symmetric), 906, 836, 683 (Polynuclear Ar.–CH out of plane bending), 976 (Ar–Cl)	δ 8.75 (s, 1H, SO_2NH), δ 7.49–8.23 (m, 6H, H-2′, H-3′, H-6′, H-7′, H-8′, H-9′), δ 6.61 (m, 1H, CONH-1), δ 5.53 (m, 1H, CONH-5), δ 3.60 (m, 1H, H-2), δ 3.16–3.20(m, 2H, N–CH_2-1″), δ 2.83–2.95 (m, 2H, N–CH_2-1‴), δ 2.23 (m, 2H, H_2-4), δ 2.04 (m, 1H, H_A-3), δ 1.78 (m, 1H, H_B-3), δ 1.45–1.55 (m, 2H, N–CH_2-2″), δ 1.24–1.12 (m, 2H, N–CH_2-2‴), δ 0.96–0.91 (m, 3H, N–CH_3-3″), δ 0.68–0.73 (m, 3H, N–CH_3-3‴)	55.51/55.78	5.95/5.87	9.25/9.54
32	$M + H^+$ peak at m/z 454	3296 (N–H str. of CONH), 3083 (Ar C–H str.), 2971 (ali C–H str.), 1643 (C═O str. of CONH), 1550 (N–H str of CONH), 1454 (Ar–C═CH str.), 1329 (S═O str of SO_2NH, asymmetric), 1159 (S═O str of SO_2NH, symmetric), 837, 763, 681 (Polynuclear Ar. –CH out of plane bending)	δ 8.77 (s, 1H, SO_2NH), δ 7.61–8.42 (m, 6H, H-2′, H-3′, H-6′, H-7′, H-8′, H-9′) δ 6.35 (m, 1H, CONH-1), δ 5.50 (m, 1H, CONH-5), δ 4.02–4.09 (m, 1H, N–CH-1″), δ 3.66–3.72 (m, 1H, N–CH-1″), δ 3.61 (m, 1H, H-2), δ 2.23 (m, 2H, H_2-4), δ 2.04 (m, 1H, H_A-3), δ 1.78 (m, 1H, H_B-3), δ 1.24–1.14 (m, 6H, CH_3-2″, CH_3-2‴·), δ 0.83–0.75 (m, 6H, CH_3-3″, CH_3-3‴)	55.51/55.65	5.95/5.76	9.25/9.65
33	$M + H^+$ peak at m/z 482	3309 (N–H str of CONH), 3087 (Ar C–H str.), 2977, 2935 (ali C–H str.), 1642 (C═O str. of CONH), 1552(N–H bend of CONH), 1436 (Ar C═CH str), 1323 (S═O str of SO_2NH, asymmetric), 1159 (S═O str of SO_2NH, symmetric), 803, 768, 678 (Polynuclear-CH out of plane bending),	δ 8.77 (s, 1H, SO_2NH), δ 7.49–8.21 (m, 6H, H-2′, H-3′, H-6′, H-7′, H-8′, H-9′), δ 5.58 (m, 1H, CONH-1), δ 5.34 (m, 1H, CONH-5), δ 3.67 (m, 1H, H-2), δ 3.28–3.30(m, 2H, N–CH_2-1″), δ 2.90–2.96 (m, 2H, N–CH_2-1‴), δ 2.31 (m, 2H, H_2-4), δ 2.10–2.19 δ (m, 4H, N–CH_2-2″, N–CH_2-2‴), δ 2.07 (m, 1H, H_A-3), δ 1.89–1.90 (m, 4H, N–CH_2-3″, N–CH_2-3‴), δ 1.13–1.18 (m, 3H, N–CH_3-4″), δ 0.73–0.78 (m, 3H, N–CH_3-4‴)	57.26/57.67	6.43/6.76	8.71/8.46
34	$M + H^+$ peak at m/z 482	3297 (N–H str. of CONH), 3093 (Ar C–H str.), 2958 (ali C–H str.), 1646 (C═O str of CONH), 1556 (NH bend of CONH), 1440 (Ar–C═CH str.), 1320 (S═O str. of SO_2NH, asymmetric), 1153 (S═O str. of SO_2NH, symmetric), 911, 835, 759, 682 (Polynuclear Ar.–CH out of plane bending);	δ 8.76 (s, 1H, SO_2NH), δ 7.61–8.42 (m, 6H, H-2′, H-3′, H-6′, H-7′, H-8′, H-9′), δ 6.71 (m, 1H, CONH-1), δ 5.58 (m, 1H, CONH-5), δ 3.63 (m, 1H, H-2), 3.02 (m, 2H, NH–CH_2-1″), δ 2.76 (m, 2H, NH–CH_2-1‴), δ 2.27 (m, 2H, H_2-4), δ 2.04 (m, 1H, H_A-3), δ 1.86 (m, 1H, H_B-3), δ 1.70–1.86 (m, 2H, NH–CH_2–CH-2″, NH–CH_2–CH-2‴), δ 0.90–0.92 (d, 6H, CH_3-4″, CH_3-4‴), δ 0.70–0.72 (d, 2H, CH_3-3″, CH_3-3‴)	57.26/56.98	6.43/6.23	8.71/8.98
35	$M + H^+$ peak at m/z 538	3296 (N–H str. of CONH), 3092 (Ar C–H str.), 2962 (ali C–H str.), 2874 (ali CH str), 1647 (C═O str. of CONH), 1556 (N–H bend of CONH), 1439 (Ar C═C str), 1328 (S═O str. of SO_2NH, asymmetric), 1153 (S═O str. of SO_2NH, symmetric), 909, 762, 682 (Polynuclear Ar.–CH out of plane bending)	δ 8.30 (1H, SO_2NH), δ 7.54–7.90 (m, 6H, H-2′, H-3′, H-6′, H-7′, H-8′, H-9′), δ 6.77 (m, 1H, CONH-1), δ 5.57 (m, 1H, CONH-5), δ 3.64 (m, 1H, H-2), δ 3.21–3.33 (m, 2H, NH–CH_2-1″), δ 3.03–3.09 (m, 2H, NH–CH_2-1‴), δ 2.29 (m, 2H, H_2-4), δ 1.98–2.00 (m, 1H, H_A-3), δ 1.86–1.91 (m, 1H, H_B-3), δ 0.83–1.63 (m, 22H, CH_2-2″, CH_2-3″, CH_2-4″, CH_2-5″, CH_2-6″, CH_2-2‴, CH_2-3‴, CH_2-4‴, CH_2-5‴, CH_2-6‴)	60.26/60.45	7.28/7.57	7.82/7.92
36	$M + H^+$ peak at m/z 550	3293 (N–H str. of CONH), 3083 (Ar C–H str.), 2929 (ali C–H str.), 1647 (C═O str. of CONH), 1550 (N–H bend of CONH), 1442 (Ar C═CH str.), 1323 (S═O str. of SO_2NH, asymmetric), 1150 (S═O str. of SO_2NH, symmetric), 887, 834, 757, 680 (Polynuclear and mononuclear Ar.–CH out of plane bending);	8.72 (s, 1H, SO_2NH), δ 7.29–8.35 (m, 11H, H-2′, H-3′, H-5′, H-6′, H-7′, H-8′, H-2″, H-3″, H-4″, H-5″, H-6″), δ 6.93 (m, 1H, CONH-1), δ 5.82 (m, 1H, CONH-5), δ 4.04–4.41 (m, 4H, NH–CH_2-1″, NH–CH_2-1‴), δ 3.70 (m, 1H, H-2), 2.29 (m, 2H, H_2-4), δ 2.03 (m, 1H, H_A-3), δ 1.77–1.84 (m, 1H, H_B-3)	63.35/63.56	5.10/5.45	7.64/7.87

(*continued on next page*)

Table 7 (*continued*)

Cpd	Mass (FAB)	IR (KBr, cm^{-1})	^1H NMR (300MHz, $CDCl_3$))	C, H, N % calcd/found		
				C	H	N
37	$M + H^+$ peak at *m/z* 414	3473 (Asymmetric N–H str. of $CONH_2$), 3375 (Symmetric N–H str. of $CONH_2$), 3178 (Ar C–H str.), 2861 (ali C–H str.), 1668 (C═O str. of $CONH_2$), 1500, 1423 (Ar–C═CH str), 1313 (S═O str of SO_2NH, asymmetric), 1137 (S═O str. of SO_2NH, symmetric), 831, 758, 679 (Polynuclear-CH out of plane bending)	δ 8.73 (s, 1H, SO_2NH), δ 7.32–8.23 (m, 6H, H-2′, H-3′, H-6′, H-7′, H-8′, H-9′), δ 5.85 (m, 2H, $CONH_2$-1), δ 5.34 (m, 2H, $CONH_2$-5), δ 3.67 (m, 1H, H-2), δ 2.27 (m, 2H, H_2-4), δ 2.01 (m, 2H, H_2-3), 1.78 (m, 1H, H_B-3)	43.44/43.08	3.86/3.97	10.14/10.35
38	$M + H^+$ peak at *m/z* 442	3315 (NH str. Of CONH), 3107 (Ar. CH Str), 2933 ali C–H str.), 1647 (C═O str. of COOH), 1556 (NH bend of CONH), 1458,1436, 1413 (Ar. C═CH str), 1357 (S═O str. of SO_2NH, asymmetric), 1161 (S═O str. of SO_2NH, symmetric), 802, 767, 680 (Polynuclear-CH out of plane bending)	δ 8.73 (s, 1H, SO_2NH), δ 7.50–8.23 (m, 6H, H-2′, H-3′, H-6′, H-7′, H-8′, H-9′), δ 6.71 (m, 1H, CONH-1), δ 5.61 (m, 1H, CONH-5), δ 3.61 (m, 1H, H-2), δ 2.72 (m, 3H, N–CH_3-1‴), δ 2.52 (m, 3H, N–CH_3-1″), δ 2.17 (m, 2H, H_2-4), δ 1.87 (m, 2H, H_2-3)	46.15/45.98	4.52/4.68	9.49/9.76
39	$M + H^+$ peak at *m/z* 470	3297 (N–H str. of CONH), 3099 (Ar C–H str.), 2976 (ali C–H str.), 1643 (C═O str of CONH), 1559 (NH bend of CONH), 1502, 1440 (Ar–C═CH str), 1323 (S═O str. of SO_2NH, asymmetric), 1150 (S═O str. of SO_2NH, symmetric), 887, 834, 757, 680 (Polynuclear Ar.–CH out of plane bending), 997 (Ar–Br);	δ 8.76 (s, 1H, SO_2NH), δ 7.68–8.40 (m, 6H, H-2′, H-3′, H-6′, H-7′, H-8′, H-9′), δ 6.58 (m, 1H, CONH-1), δ 5.51 (m, 1H, CONH-5), δ 3.62 (m, 1H, H-2), δ 3.24 (m, 2H, NH–CH_2-1″), δ 2.94 (m, 2H, NH–CH_2-1‴), δ 2.23 (m, 2H, H_2-4), δ 2.02 (m, 1H, H_A-3), δ 1.77 (m, 1H, H_B-3), 1.11–1.63 (m, 1H, CH_3-2″) δ 0.80–1.11 (m, 3H, CH_3-2‴)	48.51/48.76	5.11/5.34	8.94/8.93
40	$M + H^+$ peak at *m/z* 499	3294 (N–H str of CONH), 3101 (Ar C–H str.), 2960, 2871 (ali C–H str.), 1645 (C═O str. of CONH), 1558(N–H bend of CONH), 1436 (Ar C═CH str), 1319 (S═O str of SO_2NH, asymmetric), 1155 (S═O str of SO_2NH, symmetric), 800, 767, 680 (Polynuclear-CH out of plane bending)	δ 8.75 (s, 1H, SO_2NH), δ 7.49–8.23 (m, 6H, H-2′, H-3′, H-6′, H-7′, H-8′, H-9′), δ 6.61 (m, 1H, CONH-1), δ 5.53 (m, 1H, CONH-5), δ 3.60 (m, 1H, H-2), δ 3.16–3.20(m, 2H, N–CH_2-1″,), δ 2.83–2.95 (m, 2H, N–CH_2-1‴), δ 2.04 (m, 1H, H_A-3), δ 1.78 (m, 1H, H_B-3), δ 1.45–1.55 (m, 2H, N–CH_2-2″), δ 1.24–1.12 (m, 2H, N–CH_2-2‴), δ 0.96–0.91 (m, 3H, 3H, N–CH_2-3″), δ 0.68–0.73 (m, 3H, 3H, N–CH_2-3‴)	50.56/50.55	5.62/5.38	8.43/8.45
41	$M + H^+$ peak at *m/z* 555	3310, 3238 (N–H str of CONH), 3097 (Ar C–H str.), 2929, 2859 (ali C–H str.), 1642 (C═O str. of CONH), 1554 (N–H bend of CONH), 1438 (Ar C═CH str), 1341 (S═O str of SO_2NH, asymmetric), 1159 (S═O str of SO_2NH, symmetric), 835, 762, 679 (Polynuclear-CH out of plane bending)	δ 8.73 (s, 1H, SO_2NH), δ 7.32–8.23 (m, 6H, H-2′, H-3′, H-6′, H-7′, H-8′, H-9′), δ 5.85 (m, 1H, $CONH_2$-1), δ 5.34 (m, 1H, CONH-5), δ 3.67 (m, 1H, H-2), δ3.68 (m, 2H, N–CH_2-1″), δ (m, 2H, N–CH_2-1″), 3.13δ 2.27 (m, 2H, H_2-4), δ 2.01 (m, 2H, H_2-3), 1.78 (m, 1H, H_B-3), 1.56–1.29 (m, 12H, CH_2-2″, CH_2-3″, CH_2-4″, CH_2-2‴, CH_2-3‴, CH_2-4‴), 0.97–0.74 (m, 6H, CH_3-5″, CH_3-5‴)	54.10/54.65	4.71/4.72	7.57/7.76
42	$M + H^+$ peak at *m/z* 595	3293 (N–H str. of CONH), 3083 (Ar C–H str.), 2929 (ali C–H str.), 1647 (C═O str. of CONH), 1550 (N–H bend of CONH), 1442 (Ar C═CH str.), 1323 (S═O str. of SO_2NH, asymmetric), 1150 (S═O str. of SO_2NH, symmetric), 887, 834, 757, 680 (Polynuclear and mononuclear Ar.–CH out of plane bending).	δ 8.72 (s, 1H, SO_2NH), δ 7.29–8.35 (m, 11H, H-2′, H-3′, H-6′, H-7′, H-8′, H-9′, H-2″, H-3″, H-4″, H-5″, H-6″), δ 6.93 (m, 1H, CONH-1), δ 5.82 (m, 1H, CONH-5), δ 4.04–4.41 (m, 4H, NH–CH_2-1″, NH–CH_2-1‴), δ 3.70 (m, 1H, H-2), 2.29 (m, 2H, H_2-4), δ 2.03 (m, 1H, H_A-3), δ 1.77–1.84 (m, 1H, H_B-3)	58.53/58.67	4.71/4.87	7.06/7.32
43	$M + H^+$ peak at *m/z* 546	3294 (N–H str. of CONH), 3092 (Ar C–H str.), 2955, 2870 (ali C–H str.), 1650 (C═O str. of CONH), 1552 (N–H bend of CONH), 1458 (Ar C═CH str.), 1331 (S═O str. of SO_2NH, asymmetric), 1094, 1062 (C–O str. of C–OCH_3), 819, 752, 641 (Polynuclear Ar.–CH out of plane bending).	δ 8.72 (s, 1H, SO_2NH), δ 7.29–8.35 (m, 11H, H-3′, H-4′, H-6′, H-7′, H-8′, H-9′, H-2″, H-3″, H-4″, H-5″, H-6″), δ 6.93 (m, 1H, CONH-1), δ 5.82 (m, 1H, CONH-5), δ 4.18–4.41 (m, 4H, NH–CH_2-1″, NH–CH_2-1‴), δ 4.05 (s, 3H, OCH_3), δ 3.70 (m, 1H, H-2), 2.29 (m, 2H, H_2-4), δ 2.03 (m, 1H, H_A-3), δ 1.77–1.84 (m, 1H, H_B-3)	65.97/65.65	5.86/5.76	7.70/7.87
44	$M + H^+$ peak at *m/z* 529	3306, 3239 (N–H str. of CONH), 3074 (Ar C–H str.), 2929 (ali C–H str.), 1649 (C═O str of CONH), 1545 (NH bend of CONH), 1443 (Ar–C═CH str.), 1378 (S═O str. of SO_2NH, asymmetric), 1150 (S═O str. of SO_2NH, symmetric), 1073 (C–O str. of C–OCH_3), 804	δ 8.73 (s, 1H, SO_2NH), δ 7.32–8.23 (m, 6H, H-3′, H-4′, H-6′, H-7′, H-8′, H-9′), δ 5.85 (m, 1H, $CONH_2$-1), δ 5.34 (m, 1H, CONH-5), δ 4.06 (s, 3H, OCH_3), δ 3.67 (m, 1H, H-2), δ 2.27 (m, 2H, H_2-4), δ 2.01 (m, 2H, H_2-3), 1.78 (m, 1H, H_B-3), δ 1.05–1.93 (m, 22H, Cyclohexyl protons).	63.52/60.01	7.37/6.93	7.94/7.69
45	$M + H^+$ peak at *m/z* 533	3307, 3238 (N–H str. of CONH), 3074 (Ar C–H str.), 2929 (ali C–H str.), 1649 (C═O str of CONH), 1555 (NH bend of CONH), 1448 (Ar–C═CH str.), 1323 (S═O str. of SO_2NH, asymmetric), 1159 (S═O str. of SO_2NH, symmetric), 1073 (C–O str. of C–OCH_3), 809, 690 (Polynuclear Ar.–CH out of plane bending).	δ 8.30 (1H, SO_2NH), δ 7.40–7.91 (m, 6H, H-3′, H-4′, H-6′, H-7′, H-8′, H-9′), δ 6.77 (m, 1H, CONH-1), δ 5.57 (m, 1H, CONH-5), δ 4.08 (s, 3H, OCH_3), δ 3.64 (m, 1H, H-2), δ 3.21–3.33 (m, 2H, NH–CH_2-1″), δ 3.03–3.09 (m, 2H, NH–CH_2-1‴), δ 2.29 (m, 2H, H_2-4), δ 1.98–2.00 (m, 1H, H_A-3), δ 1.86–1.91 (m, 1H, H_B-3), δ 0.83–1.63 (m, 22H, CH_2-2″, CH_2-3″, CH_2-4″, CH_2-5″, CH_2-6″, CH_2-2‴, CH_2-3‴, CH_2-4‴, CH_2-5‴, CH_2-6‴)	62.92/59.36	7.58/7.41	7.87/6.75

0.1 kcal/Å mol. Dragon software [42] was utilized for the calculation of different topological and constitutional descriptors. The topological descriptors used are information content index (neighborhood symmetry of 0-order) (*IC*0), structural information content (neighborhood symmetry of 0-order) (*SIC*0), information content index (neighborhood symmetry of 1-order) (*IC*1), structural information content (neighborhood symmetry of 1-order) (*SIC*1), information content index (neighborhood symmetry of 2-order) (*IC*2), structural information content (neighborhood symmetry of 2-order) (*SIC*2), information content index (neighborhood symmetry of 3-order) (*IC*3), structural information content (neighborhood symmetry of 3-order), (*SIC*3) information content index (neighborhood symmetry of 4-order) (*IC*4), structural information content (neighborhood symmetry of 4-order) (*SIC*4), information content index (neighborhood symmetry of 5-order) (*IC*5) and structural information content (neighborhood symmetry of 5-order) (*SIC*5) [43–45]. The constitutional descriptors are mean atomic van der Waals volume scaled on carbon atom (*Mv*), mean atomic Sanderson electronegativity scaled on carbon atom (*Me*), mean atomic polarizability scaled on carbon atom (*Mp*), mean electrotopological state (*Ms*), rotatable bond fraction (*RBF*), number of chlorine atoms (*n*Cl) and number of bromine atom (*n*Br) [46]. Electronic descriptor Wang-Ford charge was calculated by Chem 3D Pro package [47]. The general structure of these compounds was drawn first in Chem draw ultra ver 5.0. It was saved as the template structure. This template structure was modified to draw all structures given in the dataset and saved. The numberings of atoms were done according to that of ETSA and RTSA models. To create 3-D models, all these structures were transformed to Chem 3D ver 5.0. Finally the model was cleaned up. Energy minimization was done under MOPAC module using RHF (restricted Hartee-Fock: closed shell) wave function. The energy minimized geometry was used to calculate Wang-Ford charges. Multiple linear regression analysis was performed by the computer program 'Multiregress'[48] developed in our laboratory.

Acknowledgements

The authors are grateful to All India Council for Technical Education (AICTE), New Delhi for awarding a research project. Authors are also thankful to the authority of Jadavpur University for their help and encouragement.

Appendix. Supplementary material

Supplementary data associated with this article can be found in the on-line version, at doi:10.1016/j.ejmech.2010.01.008.

References

[1] L.D. Nelson, M.M. Cox, Lehninger Principles of Biochemistry, fourth ed. W.H. Freeman, New York, 2005.
[2] M.A. Medina, J. Nutr. 131 (2001) 2539S–2542S.
[3] E.E. Conn, P.K. Stumpf, G. Bruening, R.H. Doi, Outlines of Biochemistry, fifth ed. John Wiley and Sons, New York, 2006.
[4] V.S. Klimberg, J.L. McClellan, Am. J. Surg. 172 (1996) 418–424.
[5] W.W. Souba, Ann. Surg. 218 (1993) 715–716.
[6] P. Bhattacharya, P. Maity, Pathol. Oncol. Res. 6 (2000) 217–223.
[7] A. Turner, J. McGivan, Biochem. J. 370 (2003) 403–410.
[8] B.P. Bode, B.C. Fuchas, B.P. Hurley, J.L. Conroy, J.E. Suetterlin, K.K. Tanabe, D.B. Rhoads, S.F. Abcouwer, W.W. Souba, Am. J. Physiol. Gastrointest. Liver Physiol. 283 (2002) G1062–G1067.
[9] C.L. Collins, M. Wasa, W.W. Souba, S.F. Abcouwer, J. Cell. Physiol. 176 (1998) 166–178.
[10] M.M. Ramos Lima, M.A. de Mello, R. Curi, Cell Biochem. Funct. 20 (2002) 107–111.
[11] C. Costa, J.F. Huneau, D. Tome, Biochem. Biophys. Acta 1509 (2000) 95–102.
[12] J.C. Aledo, E. de Pedro, P.M. Gomez-Fabre, I.N. Nunez de Castro, J. Marquez, Anticancer Res. 20 (2000) 1463–1467.
[13] P. Bhattacharya, S. Sett, P. Maity, J. Exp. Clin. Cancer Res. 20 (2001) 599–604.
[14] T. Matsuno, I. Goto, Cancer Res. 52 (1992) 1192–1196.
[15] M.K. Chen, R.M. Salloum, T.R. Austgen, J.B. Bland, K.I. Bland, E.M. Copeland, W.W. Souba, J. Parenter. Enteral. Nutr. 15 (1991) 159–163.
[16] K. Srikanth, C.A. Kumar, D. Goswami, A.U. De, T. Jha, Indian J. Biochem. Biophys. 38 (2001) 120–123.
[17] K. Srikanth, B. Debnath, T. Jha, Bioorg. Med. Chem. 10 (2002) 1841–1854.
[18] K. Srikanth, C.A. Kumar, B. Ghosh, T. Jha, Bioorg. Med. Chem. 10 (2002) 2119–2131.
[19] B. Debnath, K. Srikanth, S. Banerjee, T. Jha, Internet Electron. J. Mol. Des. 1 (2002) 488–502.www.biochempress.com.
[20] S. Samanta, K. Srikanth, S. Banergee, B. Debnath, S. Gayen, T. Jha, Bioorg. Med. Chem. 12 (2004) 1413–1423.
[21] S. Gayen, B. Debnath, S. Samanta, B. Ghosh, A. Basu, T. Jha, Internet Electron. J. Mol. Des. 4 (2005) 556–578.www.biochempress.com.
[22] B. Debnath, S. Gayen, S. Samanta, A. Basu, B. Ghosh, T. Jha, Indian J. Chem. 45A (2006) 93–106.
[23] S. Samanta, S.M. Alam, P. Panda, T. Jha, Eur. J. Med. Chem. 44 (2009) 70–82.
[24] J.T. Leonard, K. Roy, Bioorg. Med. Chem. Lett. 16 (2006) 4467–4474.
[25] A.K. Halder, N. Adhikary, T. Jha, Bioorg. Med. Chem. Lett. 19 (2009) 1737–1739.
[26] R. Franke, The Theoretical Drug Design Methods, first ed. Elsevier, Amsterdam, 1984.
[27] K. Roy, I. Sanyal, P.P. Roy, QSAR. Env. Res 17 (2006) 563–582.
[28] J.T. Leonard, K. Roy, Bioorg. Med. Chem. 14 (2006) 1039–1045.
[29] S.M. Alam, S. Samanta, A.K. Halder, S. Basu, T. Jha, Can. J. Chem. 85 (2007) 1053–1058.
[30] H. Hall, B. Mohney, L.B. Kier, Quant. Struct. Act. Relat. 10 (1991) 43–49.
[31] C. de Gregorio, L.B. Kier, L.H. Hall, J. Comput. Aided Mol. Des. 12 (1998) 557–561.
[32] K. Roy, A.U. De, C. Sengupta, Drug Des. Discov. 18 (2002) 33–39.
[33] B. Debnath, S. Samanta, S. Gayen, A. Basu, B. Ghosh, T. Jha, Internet Electron. J. Mol. Des. 4 (2005) 393–405. www.biochempress.com.
[34] B. Debnath, S. Gayen, A. Basu, K. Srikanth, T. Jha, J. Mol. Model. 10 (2004) 328–334.
[35] S. Samanta, B. Debnath, A. Basu, K. Srikanth, S. Gayen, T. Jha, Eur. J. Med. Chem. 41 (2006) 1190–1195.
[36] A.K. Ghose, A. Pritchett, G.M. Crippen, J. Comput. Chem. 9 (1988) 80.
[37] R. Carrasco, A.J. Padron, J. Galvez, J. Pharm. Pharm. Sci. 7 (2004) 19.
[38] S. Samanta, B. Debnath, S. Gayen, B. Ghosh, K. Srikanth, A. Basu, T. Jha, Il Farmaco. 60 (2005) 818.
[39] S. Samanta, S.M. Alam, P. Panda, T. Jha, Internet Electron. J. Mol. Des. 5 (2006) 503. www.biochempress.com.
[40] Mouse is a computer program developed by Jadavpur University.
[41] Hypercube, Inc. Hyperchem Professional Release 7.0 [Computer Program]. Hypercube Inc., Gainesville, Florida, 2002.
[42] DRAGON web version 2.1 is a QSAR software developed by Milano Chemometrics and QSAR Research Group, Dipartimento di Scienze dell'Ambiente e del Territorio Universitàdegli Studi di Milano – Bicocca.
[43] D. Bonchev, Information Theoretic Indices for Characterization of Chemical Structures. RSP-Wiley, UK, 1983.
[44] V.R. Magnuson, D.K. Harriss, S.C. Basak, in: R.B. King (Ed.), Studies in Physical and Theoretical Chemistry, Elsevier, Amsterdam, 1983, pp. 178–191.
[45] S.C. Basak, G.D. Gute, SAR. QSAR. Environ. Res. 7 (1997) 1–4.
[46] R. Todeschini, V. Consonni, Handbook of Molecular Descriptors, first ed. Wiley, Weinheim, 2000.
[47] Chem 3D Pro Version 5.0 and Chem Draw Ultra Version 5.0 are programs of CambridgeSoft Corporation, U.S.A.
[48] Multi Regress is a software developed by Jadavpur University.